ELECTRIC BIREFRINGENCE STUDY OF RABBIT SKELETAL MYOSIN SUBFRAGMENTS

HMM, LMM, and Rod in Solution

R. CARDINAUD* AND J. C. BERNENGO‡
*Service de Biophysique, CEN Saclay, 91191 Gif-sur-Yvette Cedex, France; and
‡Laboratoire de Génie Biologique et Médical, Faculté de Médecine, 25030 Besançon, France

SUMMARY

Electric birefringence measurements and depolarized light scattering experiments were performed with HMM, LMM, and rod, the three fragments of myosin, under conditions (0.3 M KCl, 0.02 M PO_4, pH 7.3) the medium currently used for biochemical assays of myosin in its native state as well as of its subfragments. The comparison of myosin and rod relaxation times (17.2 and 22.8 μs, respectively) suggests that the average bend angle in the tail is sharper in intact myosin (90°) whereas rod, when detached from the heads, is a more elongated species with an average bend angle of 120–135°. The LMM relaxation time (6.4 μs) is consistent with a rigid linear stick model of length 78 nm. Flexibility in myosin tail is thus confirmed as located in the HMM-LMM hinge.

LMM and rod did not exhibit any significant variation of their apparent relaxation times with concentration and the decay curves were best fitted by a single exponential, evidence that the concentration of parallel staggered dimers was negligible in the concentration range studied here (0–7 g/l). This observation lends support to previous results obtained with myosin.

Respective HMM, LMM, and rod molecular weights and homogeneity as evaluated by SDS-PAGE analysis were correlated to the Kerr constants of their solutions. Large variations in LMM Kerr constants could be related to the loss of a COOH-terminal peptide on prolonged chymotryptic digestion. Electric birefringence combined with depolarized light scattering is presented as a potential method for net charge distribution studies.

INTRODUCTION

Fast skeletal muscle myosin is composed of two heavy chains and four light chains organized in a typically asymmetric structure (for a review see Lowey, 1971; Harrington, 1979). A long helical coiled coil (the tail) incudes about three-fifths of the two heavy chains (M_r = 200 k) intertwined on their COOH-terminal side. The rest of each heavy chain forms an oblong head, the exact shape of which is not precisely known. Each head carries two light chains; one is the so-called Nbs2 or phosphorylatable light chain (or LC-2, M_r = 19 k), while the other is either an A-1 light chain (LC-1, M_r = 21 k) or an A-2 light chain (LC-3, M_r = 17 k). In rabbit fast skeletal muscle the ratio of A-1 to A-2 is 2/1.

This complex and highly asymmetric myosin molecule can be physically separated by digestion of myosin with such proteolytic enzymes as trypsin, papain, or chymotrypsin. Proteolytic digestion and products thereof have been the matter of extensive biochemical studies. Heavy meromyosin (HMM)[1] obtained by tryptic or chymotryptic digestion contains the functional ATPase and actin binding sites, both more precisely located in the two (equivalent ?) globular heads. These heads are attached at the NH_2-terminal extremity of S-2, a part of the tail containing on its COOH-terminal region a functionally essential flexible zone. The other product in tryptic or chymotryptic digestion, light meromyosin (LMM), represents the rest of the α-helical coiled-coil tail. This LMM was found to be involved in the assembly of myosin molecules to form the thick filament (Lowey, 1971).

In a previous electric birefringence study (Bernengo and Cardinaud, 1982) it was shown that rabbit skeletal myosin is mainly present in monomer form at high ionic strength. The experimental results were best accounted for by a myosin molecule model bent in its rod portion with a bend angle of ~90°. This shape differs from the usual schematic picture of the myosin monomer in which the tail

[1] *Abbreviations used in this paper:* EDTA, ethylene dinitrilotetraacetic acid; Nbs2, 5,5-dithiobis-(2-nitrobenzoic acid); HMM, heavy meromyosin; LMM, light meromyosin; S-2, HMM-subfragment-2; CT, chymotrypsin; T, trypsin; PAGE, polyacrylamide gel electrophoresis; SDS, sodium dodecyl sulfate; DEAE, dimethylaminoethyl. Because of the influence of preparative methods on the structure of such typical myosin subfragments as HMM, LMM, rod, etc., these subfragments are characterized in the following way: information given in brackets before the name of the fragment refers to its origin, i.e., the conditions under which it was obtained e.g., (5 min, Ca^{2+}, CT)-HMM defines an HMM species obtained by a 5 min chymotryptic digestion in the presence of Ca^{2+}.

BIOPHYS J. © Biophysical Society · 0008-3495/85/10/751/13 $1.00
Volume 48 October 1985 751–763

is represented as an extended rigid stick. Electron microscope images (Elliott and Offer, 1978; Takahashi, 1978) and a number of hydrodynamic (Harvey and Cheung, 1977) and other physical studies (Highsmith et al., 1977; Kobayasi and Totsuka, 1975; Miyahara and Noda, 1979) suggest a certain degree of flexibility all along the rod with a definitely more flexible zone at the HMM-LMM junction.

Alternatively, therefore, the behavior of myosin in solution as observed by electric birefringence could conceivably be explained by the flexibility of the molecule at the HMM-LMM hinge. In this alternative explanation the HMM part only would be rapidly oriented when the electric field is applied and the recorded relaxation time could no longer be used to compute a value of the average bend angle in the tail of intact myosin. Our preliminary experiments with HMM (Bernengo and Cardinaud, 1982) yielded relaxation signals that seemed to exclude this interpretation, but further studies on the various available myosin fragments were needed to provide: (*a*) molecular parameters such as lengths and average shapes of myosin and its subfragments in solution for a more precise description of the characteristics of the hinge (see, e.g., Highsmith, 1981), an important feature in the cross-bridge/sliding filament model (Huxley, 1963, 1969; Huxley and Simmons, 1971) of muscular contraction; (*b*) confirmatory evidence that myosin is mostly present as monomer in high ionic strength media as indicated in our previous study, whereas other reports indicate a strong tendency for myosin to autoassociate into dimers (Godfrey and Harrington, 1970; Herbert and Carlson, 1971; Harrington and Burke, 1972).

Here the preparation and biochemical characteristics of HMM, LMM, and rod are correlated to the Kerr constant of their solution. Variations according to preparation conditions were observed in Kerr constants but not in relaxation times, showing the great sensitivity of this electrooptical method in detecting cleavages severing even very small fragments at either side of such elongated species. Relaxation times were used to calculate the length of the various myosin subfragments. The LMM length was first calculated from Broersma's equation for cylindrical macromolecules and compared with values obtained by several other technical approaches. The length of S-2 (the complementary part in rod) was derived from HMM electric birefringence measurements through the Garcia de la Torre and Bloomfield model. The rod length is therefore the sum of LMM and S-2, assuming no overlap or missing piece between the two fragments when LMM and HMM are prepared. Introduced into Broersma's equation, this value yielded a rotational diffusion coefficient significantly different from the one determined by electric birefringence. A reasonable explanation as put forward earlier by Highsmith et al. (1977) is that rod presents a bend at the S-2–LMM junction at high pH (9.5), as well as under our own conditions (pH 7.3). The average bend angle was calculated at 120–135°. From the nonlinearity of $\Delta n = f(c)$ observed with rod at higher concentrations an estimate of the putative autoassociation phenomenon is presented and compared with values obtained earlier by independent methods (Harrington and Burke, 1972).

MATERIAL AND METHODS

Protein Preparations

Myosin. Myosin was extracted from the back muscle of rabbit as described earlier (Cardinaud, 1979), with three precipitation cycles at low ionic strength. All operations were carried out at 2–4°C unless otherwise stated. Myosin was further purified by the Godfrey and Harrington (1970) procedure as described in a previous study. (Cardinaud and Drifford, 1982). The fraction precipitated between 40 and 45% ammonium sulfate saturation (adjusted to pH 6.75 with 10 mM EDTA) was dissolved in 0.177 (vol/wt) 3 M NaCl and diluted to stock solution concentration (usually 10–12 mg/ml) with the appropriate buffer.

HMM. HMM was prepared from purified myosin by chymotryptic digestion (Weeds and Taylor, 1975) at high ionic strength in the presence of Ca^{2+}, essentially as described (Cardinaud, 1979). Purified myosin was dissolved in 0.6 M NaCl, 0.02 M PO_4 (pH 7.0); $CaCl_2$, at final concentration 2 mM, was added just before digestion. Digestion was carried out with α-chymotrypsin, 0.03 mg/ml, at 23–24°C for various times as indicated in Results. After dialysis overnight against 0.3 NaCl, 0.02 M PO_4, 0.01 M EDTA, pH 7.0, the precipitate was removed by centrifugation (crude LMM fraction) and the supernatant again dialyzed against 0.025 M Imidazole-HCl, pH 7.0, then placed on a column (1.9 × 45 cm) of DEAE-cellulose equilibrated with the same buffer. HMM was eluted with an NaCl gradient in the same buffer (gradient slope: 0.45 mM/ml). Fractions containing HMM (checked by SDS-PAGE) were pooled and the protein was precipitated with 55% saturated ammonium sulfate containing 0.01 M EDTA, pH 6.75. After 30 min at 2–4°C the light precipitate was collected by 60 min centrifugation at 100,000 *g* then redissolved in the appropriate filtered buffer (see below).

(Ca^{2+}, CT)-LMM. The crude LMM fraction obtained after chymotryptic digestion was used to obtain purified LMM with the alcohol precipitation method described by Szent-Gyorgyi et al. (1960). The crude LMM precipitate was dissolved in 0.177 (vol/wt) 3 M NaCl then diluted with 0.5 M NaCl, and 0.01 M EDTA, pH 7.0. Three volumes of cold ethanol were slowly added within 30 min with continuous gentle stirring. The precipitate was centrifuged (15 min, 8,000 *g*) and dispersed in filtered (see below) 0.5 M KCl, dialyzed overnight against 0.3 M KCl, 0.02 M PO_4, and 0.01 M EDTA, pH 7.3 and finally centrifuged for 2 h at 100,000 *g*. The supernatant was used as stock solution for electric birefringence studies, after suitable dilution with filtered buffer and centrifugation under the same conditions.

(Ca^{2+}, T)-LMM. This species was prepared according to the same procedure, α-chymotrypsin being replaced by trypsin at 0.03 mg/ml. The reaction was stopped by soybean trypsin inhibitor (0.06 mg/ml).

(EDTA, CT)-Rod (Weeds and Taylor, 1975; Lowey et al., 1969). A myosin suspension (10–15 mg/ml) in 0.06 M NaCl, 0.02 M PO_4, and 0.01 M EDTA, pH 7.0 was digested with α-chymotrypsin (1 mg/ml dissolved in 1 mM HCl) at final concentration 0.03 mg/ml, 24°C, 8 min. The reaction was stopped by addition of PMSF at 5×10^{-4} M final concentration. S-1 and other minor soluble fragments remain in the

supernatant after centrifugation (60 min, 70,000 *g*). The pellet was dissolved in 0.177 (vol/wt) 3 M NaCl then diluted to ~20 mg/ml with a 0.5 M NaCl, 0.02 M PO_4, and 0.01 M EDTA solution at pH 7.0. The rod was purified by the procedure used for LMM. The ethanol precipitate was spun down at 8,000 *g* for 30 min, dissolved in appropriate filtered (see below) buffers and dialyzed. In some preparations it was found necessary to purify further by one or two precipitation cycles at low ionic strength. The rod solution was dialyzed against 0.03 M NaCl, and 0.02 M PO_4, pH 6.5, and the precipitate centrifuged (20,000 *g*, 30 min) then dissolved in filtered buffers as above. Diluted samples adjusted to the desired concentrations were then centrifuged again just before measurement, as described below.

Sample Preparation

As pointed out in previous reports (Cardinaud and Drifford, 1982; Bernengo and Cardinaud, 1982; see also Montague and Carlson, 1982) it is essential to use samples of the best optical quality. The samples were all dissolved and subsequently diluted with filtered (Millipore filters type VM 50 nm) buffers prepared with deionized and glass-distilled water. All samples brought to the desired concentration were centrifuged at 100,000 *g* for 2 or 3 h just before measurement and transferred directly from the centrifuge tube to the optical cuvette. All measurements were made within 5 d after myosin preparation.

Electrophoretic Analyses

SDS-PAGE was used to check the purity and characteristics of all samples under conditions described previously (Cardinaud, 1979).

Protein Measurements

Concentrations of myosin and its subfragments were determined either by the Folin-Lowry technique (as in Bailey, 1967) or by absorbance at 280/320 nm using $\epsilon^{1\%}_{280} = 5.5$ for myosin (Godfrey and Harrington, 1970), 6.0 for HMM, 2.2 for rod and 3.0 for LMM (Margossian et al., 1981).

Electric Birefringence Measurements

Electric birefringence measurements have proved feasible in media usually employed to study myosin in solution (high ionic strength: generally 0.3 M KCl). Owing to the conductivity of such solutions, the applied electric field E and the pulse length t_p must be limited to avoid excessive heating in the measurement cell. The current flowing through the sample being ~100 A, a special generator using thyristors has been designed for these experiments. The sensitivity of the photodiode detector employed in earlier experiments with collagen (Bernengo et al., 1974) has been increased, and averaging techniques have been adopted to obtain a better signal-to-noise ratio for the recording of alternate pulse responses at low fields particularly. Apart from these modifications, the basic equipment (measuring cell, laser light source, and optical bench) is very similar to the device already described (Bernengo et al., 1973).

The fundamental principles of electric birefringence applied to macromolecule solutions have already been published (Kahn, 1972; Fredericq and Houssier, 1973), and only a few equations are presented in connection with the study carried out here. These relations assume that: (*a*) the electric field actually interacting with the macromolecules is a Lorentz field; (*b*) intermolecular electrical interactions may be neglected; and (*c*) the actual electric field orienting macromolecules is equal to the applied electric field. Let us consider a cylindrical model such as a rod, with: μ, permanent dipole moment along the main axis; $\Delta\alpha_E$, difference between longitudinal and transverse polarizability; $\Delta\alpha_o$, molecular optical anisotropy factor and θ, rotary diffusion constant about a transverse axis; the steady state birefringence at limiting low fields E is then given by:

$$\Delta n_0 = \frac{2\pi N}{15nk^2T^2}\Delta\alpha_o(\mu^2 + \Delta\alpha_E kT)E^2, \qquad (1)$$

where N is the number of molecules per unit volume, n the refractive index of the solution, and k the Boltzmann constant.

A more common formulation involves the concentration c and the partial specific volume $\bar{V}$ such that

$$\Delta n = \frac{2\pi c\bar{V}}{15nk^2T^2}\cdot\frac{\Delta\alpha_o}{V}(\mu^2 + \Delta\alpha_E kT)E^2, \qquad (2)$$

where the ratio $\Delta\alpha_o/V$ is called the optical polarizability per unit volume of solute particles and may be determined without knowledge of the molecular weight M_r.

Since, as shown below, the macromolecules studied in this work are mainly polarized by permanent dipolar orientation, the term $\Delta\alpha_E kT$ vanishes compared with μ^2, which may be expressed in terms of specific Kerr constant, $K_{sp} = \Delta n/cE^2$, as

$$\mu^2 = \frac{15nk^2T^2}{2\pi\Delta\alpha_o}\cdot\frac{M_r}{\mathcal{N}}\cdot K_{sp} \qquad (3)$$

with $\mathcal{N}$ Avogadro's number.

The dynamic part of this study is quite simple, since single first-order relaxation mechanisms have been found in all solutions studied according to the decay formula

$$\Delta n = \Delta n_o \cdot e^{-t/\tau}$$

with $\tau = 1/6\,\theta$ (θ: rotary diffusion constant of the macromolecules .

Optical Anisotropy Measurements

In Eq. 1 it is clear that the electric birefringence Δn_0 is proportional to the optical anisotropy term $\Delta\alpha_0$. Any determination of the permanent or induced dipole moment of the molecules requires an evaluation of $\Delta\alpha_o$. Kobayasi and Totsuka (1975), for instance, have used a flow birefringence technique for this purpose, but the method based on Rayleigh depolarized light scattering measurements is undoubtedly the most straightforward. The experiments were performed with a "Gamma Diffusomètre" built by "Electronique Appliquée. " specially designed for measuring very low scattered intensities in pure isotropic liquids for example. The intense spectral line at 546.1 nm of a 200 W mercury arc lamp is focused through a set of lenses and pinholes at the center of the measuring cell. The horizontally polarized light scattered at 90° is compared with a small fraction of the incident light by means of a differential detector. Stray light on the wall of the cell is minimized by immersion in a benzene bath. To avoid geometric factor determinations, always tricky in light scattering experiments, relative measurements only were carried out with ultra-pure cyclohexane used as reference.

The Rayleigh factor (intensity of scattered light per unit volume and incident irradiance) for a dilute solution is given by

$$R_S = \frac{32\pi^4}{135\lambda^4}\cdot\frac{\mathcal{N}c}{M_r}\cdot(n^2+2)^2\gamma^2 + R_o \qquad (5)$$

with: λ, wave length; c, weight concentration of solute; n, refractive index of the solution; γ, molecular optical anisotropy; R_o, solvent Rayleigh factor; M_r, molecular weight of solute. For the cylindrical model assumed in relation (1)

$$\gamma^2 = (\alpha_o\,//\, - \alpha_o\perp)^2 = \Delta\alpha_o^2, \qquad (6)$$

where $\alpha_o\,//$ is the optical polarizability along the cylinder axis and $\alpha_o\perp$ that along any perpendicular axis.

In Eq. 5 several approximations have been assumed valid: (*a*) the solution is dilute enough for the solvent molar concentration to be taken as that in the pure state; (*b*) no solvent-solute interaction liable to change the Rayleigh factor of pure solvent takes place in the solution; (*c*) the actual field $\vec{F}$ acting in molecules is a Lorentz field, i.e.,: $\vec{F} = [(n^2+2)^2/9]\vec{E}$ this same assumption is already valid for Eqs. 1 and 2; and (*d*) in the absence

of more precise information the refractive index of macromolecules is considered to be the same as that of the solvent ($n = 1$ in Lorentz formula).

Owing to these assumptions, the molecular optical anisotropy is not determined rigorously. Attempts to correct experimental values according to molecular shapes and local fields are defeated by the need for some parameters usually not available with biological macromolecules (molecular refractive index for example). The above approximations will therefore be considered adequate for determination of the permanent dipole moment of the species studied here by electric birefringence. It should also be mentioned that the same types of approximation apply in the electric birefringence determinations. Combining Eqs. 2 and 3 the value of the molecular permanent dipole moment μ can be determined from birefringence and depolarized light scattering

$$\mu^2 = \frac{2\pi}{3} n (n^2 + 2) \frac{k^2 T^2}{\lambda^2} \cdot K_{sp} \cdot \left(\frac{30 c M_r}{R_S \mathcal{N}} \right)^{1/2} \qquad (7)$$

and under our experimental conditions

$$\mu^2 = 4 \cdot 10^{-29} \cdot K_{sp} \cdot \left(\frac{c M_r}{R_s} \right)^{1/2},$$

where c is the depolarized light scattering concentration.

RESULTS

HMM was prepared as described in Material and Methods and characterized systematically for purity and light chain content by SDS-PAGE. In the course of this work slight variations in the $\Delta n/cE^2$ value were observed from one preparation to another. This could be related to the observation (Cardinaud, 1979) that (Ca^{2+}, CT)-HMM SDS-PAGE patterns vary significantly with digestion time, a 137-kilodalton heavy chain predominant in the early phase of digestion being progressively replaced by one of 125 kilodaltons. HMM was therefore prepared by chymotryptic digestion for 5 min, 12 min, and 20 min. Although no clear heavy chain variation was detected by SDS-PAGE (probably because the resolution is too low in this molecular weight range) considerable changes were apparent in the light chain composition. Since the A-1 light chain is not affected by chymotryptic digestion (Weeds and Pope, 1977) the light chain content was normalized in reference to A-1 = 1.35, a standard value in our intact rabbit skeletal myosin preparations (Sarkar, 1973). After a 5-min digestion the purified HMM had a light chain ratio (A-1/Nbs2-LC/A-2) of 1.35 : 1.23 : 1.60. Evidently "A-2" is a mixture of A-2 and partially cleaved Nbs2-LC (see, e.g., Weeds and Pope, 1977; Cardinaud, 1980). After a 20-min digestion this same ratio was 1.35 : 0.45 : 2.50 (Fig. 1 *b*, *c*).

The different HMM species were studied in a 0.3 M KCl, 0.02 M PO_4, 0.01 M EDTA, pH 7.3 buffer. Although a lower ionic strength medium would also have been suitable, this buffer was chosen specially for purposes of comparison with LMM and rod measurements. Most experiments were carried out at 6°C, but a 17°C temperature was also used to relate to a previous study (Bernengo and Cardinaud, 1982). A typical birefringence response is shown on Fig. 2 *a*. The dissymmetry between the rise and decay of the signal is typical of a permanent dipole moment orientation, as already shown (Bernengo and Cardinaud, 1982) by reverse pulse experiments and confirmed by birefringence rise curve fitting. At our experimental precision the birefringence decay curves are all fitted by a monoexponential function (mean relative deviation $< 6 \cdot 10^{-4}$). An example of such a fit is given in Fig. 2 *b*. The relaxation time obtained at several applied fields with different HMM concentrations are given in Table I, which clearly shows that τ is reasonably constant under our experimental conditions and depends neither on the type of preparation (indicating in particular that digestion time has little influence on the hydrodynamic parameters of these protein species) nor on the concentration. After temperature and viscosity corrections we obtain for $\theta_{20,w}$ a value of 18,000 ± 1,000 s^{-1}.

The corresponding steady state birefringence is plotted

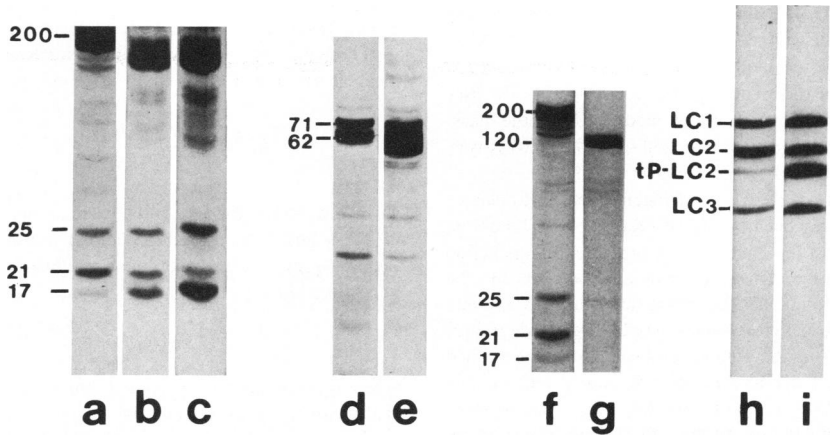

FIGURE 1 Polyacrylamide gel electrophoreses of myosin and subfragments. SDS-PAGE: (*a*) myosin; (*b*) (5 min, Ca^{2+}, CT)-HMM; (*c*) (20 min, Ca^{2+}, CT)-HMM; (*d*) (5 min, Ca^{2+}, CT)-LMM; (*e*) (20 min, Ca^{2+}, CT)-LMM; (*f*) myosin as a reference for rod; (*g*) (8 min, EDTA, CT)-rod. The various stained bands are identified by apparent molecular weights (in kilodaltons). Urea-PAGE: (*h*) a typical myosin sample showing <10% phosphorylation on LC-2; (*i*) myosin thiophosphorylated with endogenous MLCK prior to purification used as a reference for unphosphorylated myosin.

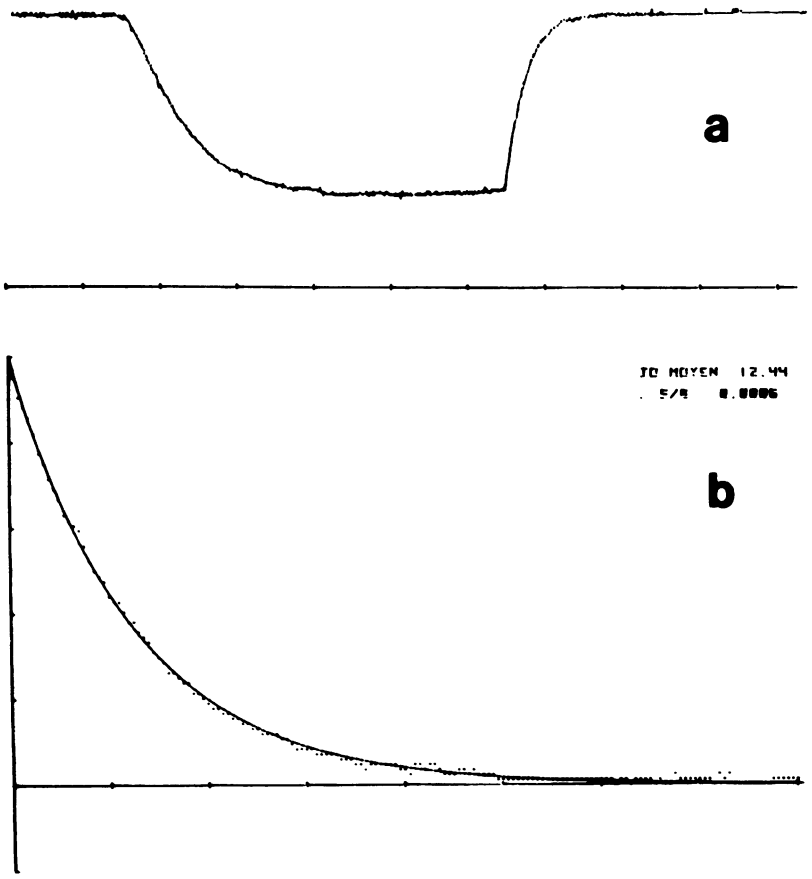

FIGURE 2 Typical birefringence signal obtained with (20 min, Ca^{2+}, CT)-HMM in 0,3 M KCl; 0,02 M PO_4; 0,01 M EDTA, pH 7.3. Concentration: 1.16 g/l; applied electric field: 650 V/cm. (*a*) complete signal, (*b*) decay and monoexponential fit with τ = 12.44 μs.

TABLE I
RELAXATION TIME OF VARIOUS HMM SPECIES AS A FUNCTION OF CONCENTRATION AND APPLIED FIELDS

Species	Concentration	Field strength	τ
	g/l	*V/cm*	*μs*
(5 min, Ca^{2+}, CT)-HMM	0.35	650	14.9
	0.75	570	13.4
	1.5	340	13.4
	1.5	570	14.1
	3.05	340	13.4
	3.05	570	13.0
	5.05	570	14.4
(20 min, Ca^{2+}; CT)-HMM	0.56	650	12.6
	2.32	340	14.0
	2.32	640	12.44
	4.65	340	13.16
	4.65	650	13.2
	7.75	260	14.0
	7.75	660	15.2
(12 min, Ca^{2+}, CT)-HMM	1.47	650	12.5
	5.95	650	13.3

Measurements at 6°C in 0.3 M KCl; 0.02 M PO_4; 0.01 M EDTA pH 7.3.

in Fig. 3 vs. concentration at several applied field strengths. These curves are all linear up to concentrations of the order of 5 g/l. At the accuracy of our experiments the Kerr law applies for all concentrations studied, as seen in Table II, which gives the values of the HMM specific Kerr constants (K_{sp}) at several concentrations and applied fields. In Fig. 3 a slight decrease in K_{sp} at high concentration is visible, particularly for (5 min, Ca^{2+}, CT)-HMM. A systematic and significant $\Delta n/c$ difference between the two preparations can be observed.

LMM

Preliminary birefrigence experiments on LMM solutions had shown large signal amplitude variations from one preparation to another, and subsequent SDS-PAGE analysis confirmed the nonhomogeneity of these preparations. A typical doublet with apparent molecular weights of 71 and 62 kilodaltons in the ratio 0.45 : 0.55 was found after a 5-min digestion, whereas a triplet (71, 62, 55 kilodaltons in ratios 0.31 : 0.49 : 0.20) was observed after a 20-min digestion (Fig. 1 *d* and *e*). The 62 and 55 kilodalton components in Fig. 1 *e* are not clearly resolved and can only be detected by densitometric analysis. The birefringence of these two preparations was studied in the same buffer as

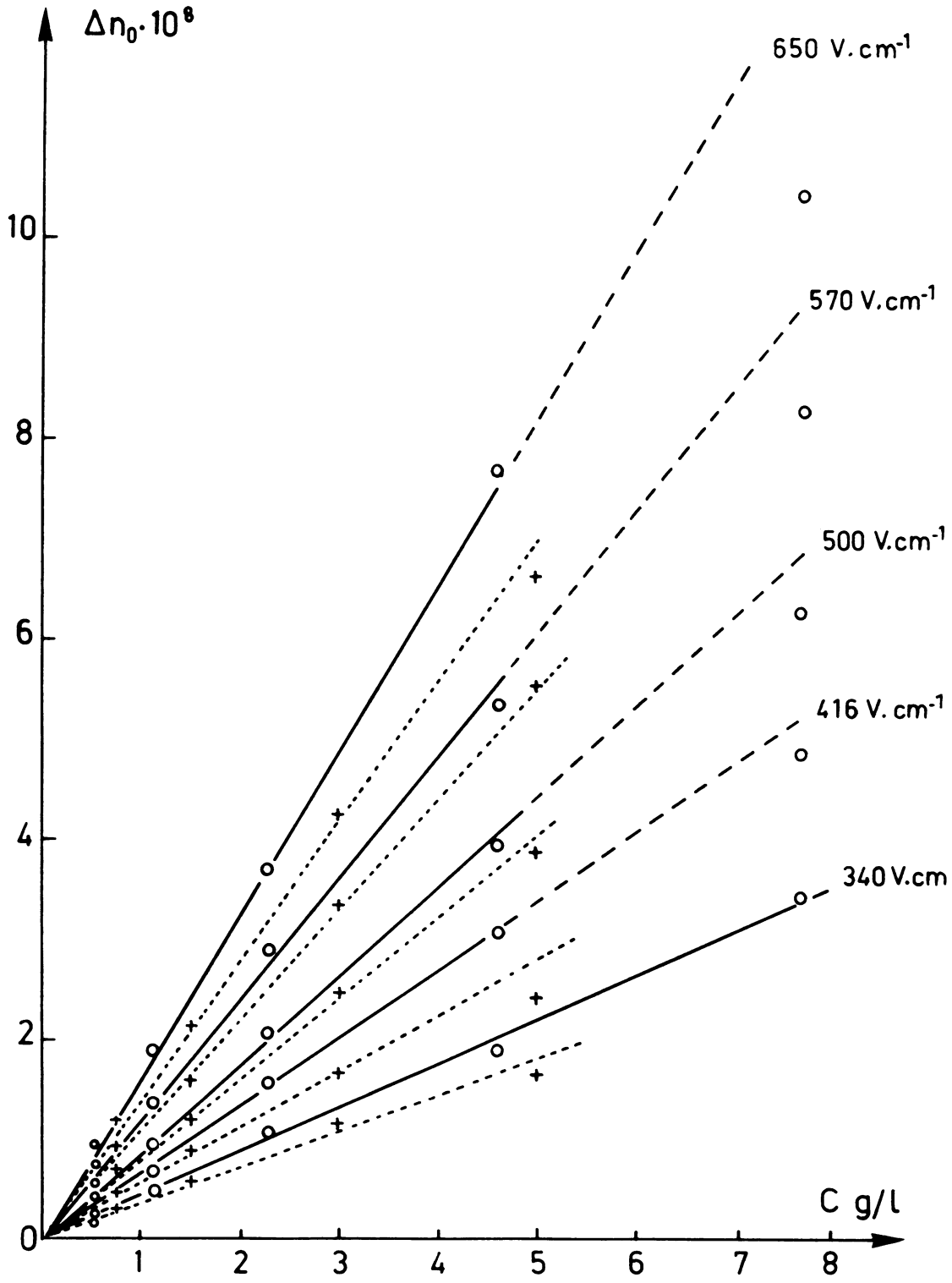

FIGURE 3 Steady state birefringence of HMM vs. concentration for various applied fields. O: (20 min, Mg, CT)-HMM; +: (5 min, Mg, CT)-HMM.

that used for HMM. A typical signal and the corresponding decay are shown in Fig. 4 *a* and *b* for (20 min, CT)-LMM samples. The molecular orientation is again due mainly to a permanent dipole moment and the disorientation process is correctly represented in any case by a single first order relaxation mechanism. No significant concentration effect was observed on the recorded relaxation time value for either (5 min, CT)- or (20 min, CT)-LMM, (see Table III). After corrections the rotary diffusion constant of LMM is $\theta_{20,w} = 26{,}000 \pm 1{,}500\ s^{-1}$.

TABLE II
SPECIFIC KERR CONSTANT AT DIFFERENT APPLIED FIELDS

Species	Concentration	Applied field in volts per centimeter				
		340 V/cm	416 V/cm	500 V/cm	570 V/cm	650 V/cm
	g/l					
(5 min, Ca^{2+}, CT)-HMM	0.35	4.2	3.5	3.8	3.4	3.6
	0.75	3.5	3.7	3.3	3.4	3.6
	1.5	3.0	3.0	2.9	2.9	3.0
	3.05	3.0	2.9	2.9	3.1	3.0
	5.05	3.6	2.5	2.8	3.0	2.8
(20 min, Ca^{2+}, CT)-HMM	0.56	3.7	4.1	3.5	3.7	3.6
	1.16	3.3	3.0	2.9	3.2	3.4
	2.32	3.4	3.5	3.2	3.5	3.9
	4.65	3.1	3.5	3.1	3.2	3.6
	7.75	1.6	1.5	1.9	1.7	2.0

Applied field (V/cm) in gram centimeter per second electrostatic unit ($\times 10^{-6}$). Measurements were carried out at 6°C in 0.3 M KCl, 0.02 M P04. 0.01 M EDTA, pH 7.3.

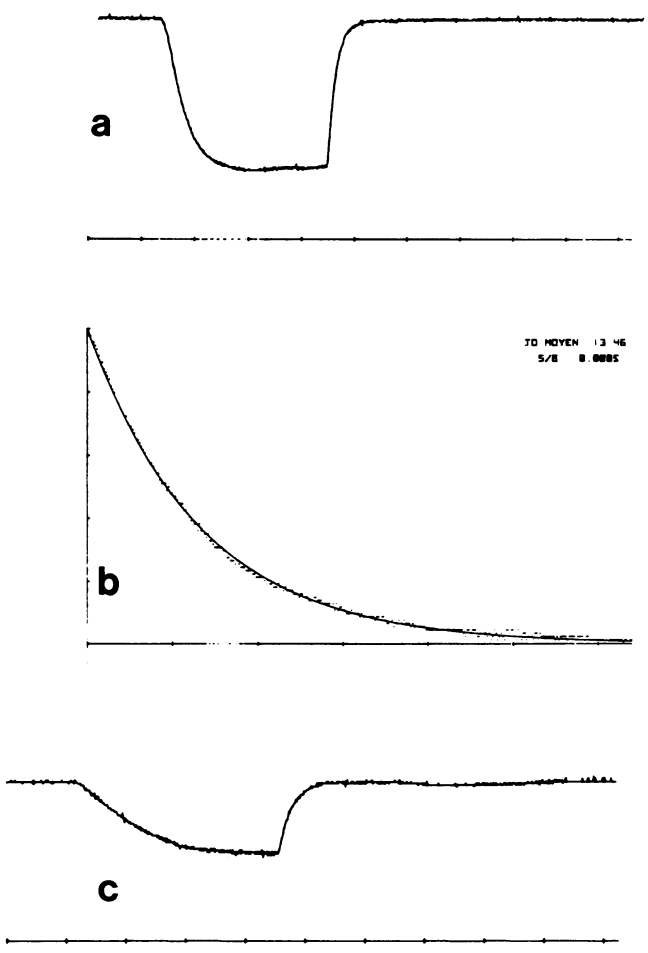

FIGURE 4 Typical birefringence signal for LMM (*a*) and decay curve (*b*). Sample was (20 min, Ca^{2+}, CT)-LMM; concentrations: 9.32 *g*/l; applied electric field: 570 V/cm. Decay and monoexponential fit with τ = 13.46 μs. (*c*) Typical birefringence signal for rod; sample was (8 min, EDTA, CT)-rod; concentration: 4 g/l; applied electric field: 280 V/cm.

Fig. 5 shows the steady state birefringence vs. concentration curves at various applied fields for both types of LMM. Good linearity is observed up to 4.2 g/l, but it is clear from both Fig. 5 and Table IV that the specific Kerr constant of (20 min, CT)-LMM is much higher than the corresponding (5 min, CT)-LMM value (typically 2.6 $\times$ 10^{-6} as compared with 0.6 $\times$ 10^{-6} c.g.s. e.s.). These two Kerr constant values were correlated more precisely with the corresponding SDS-PAGE patterns by the following experiment: a (5 min, CT)-LMM solution with a recorded K_{sp} of 0.6 $\times$ 10^{-6} (similar to a value given in Table IV for

TABLE III
RELAXATION TIMES MEASURED FOR LMM SPECIES AT VARIOUS CONCENTRATIONS

Species	Concentration	τ (μs)
	g/l	
(5 min, Ca^{2+}, CT)-LMM	1.48	9.5 ± 1
	3.33	9.3 ± 1
T = 6°C		
(5 min, Ca^{2+}, CT)-LMM	1.8	7.8 ± 5
	3.2	6.8 ± 5
T = 17°C		
(12 min, Ca^{2+}; CT)-LMM	1.07	13.0 ± 2
	5.7	10.0 ± 1
T = 6°C	9.32	10.0 ± 1
(20 min, Ca^{2+}; CT)-LMM	0.41	8.6 ± 1
	0.82	8.9 ± 1
T = 6°C	1.35	9.3 ± 0.5
	2.85	9.8 ± 0.3
	4.26	10.6 ± 0.2
(8 min, EDTA, CT)-rod	0.35	25.0 ± 5[a]
	0.70	24.3 ± 2[a]
T = 17°C	0.70	23.0 ± 3[b]
	2.33	25.5 ± 1[b]
	2.33	27.0 ± 1[c]

Applied field, 650 V/cm; conditions as in Table I, except for rod where it was (*a*) 545 V/cm; (*b*) 410 V/cm; (*c*) 280 V/cm.

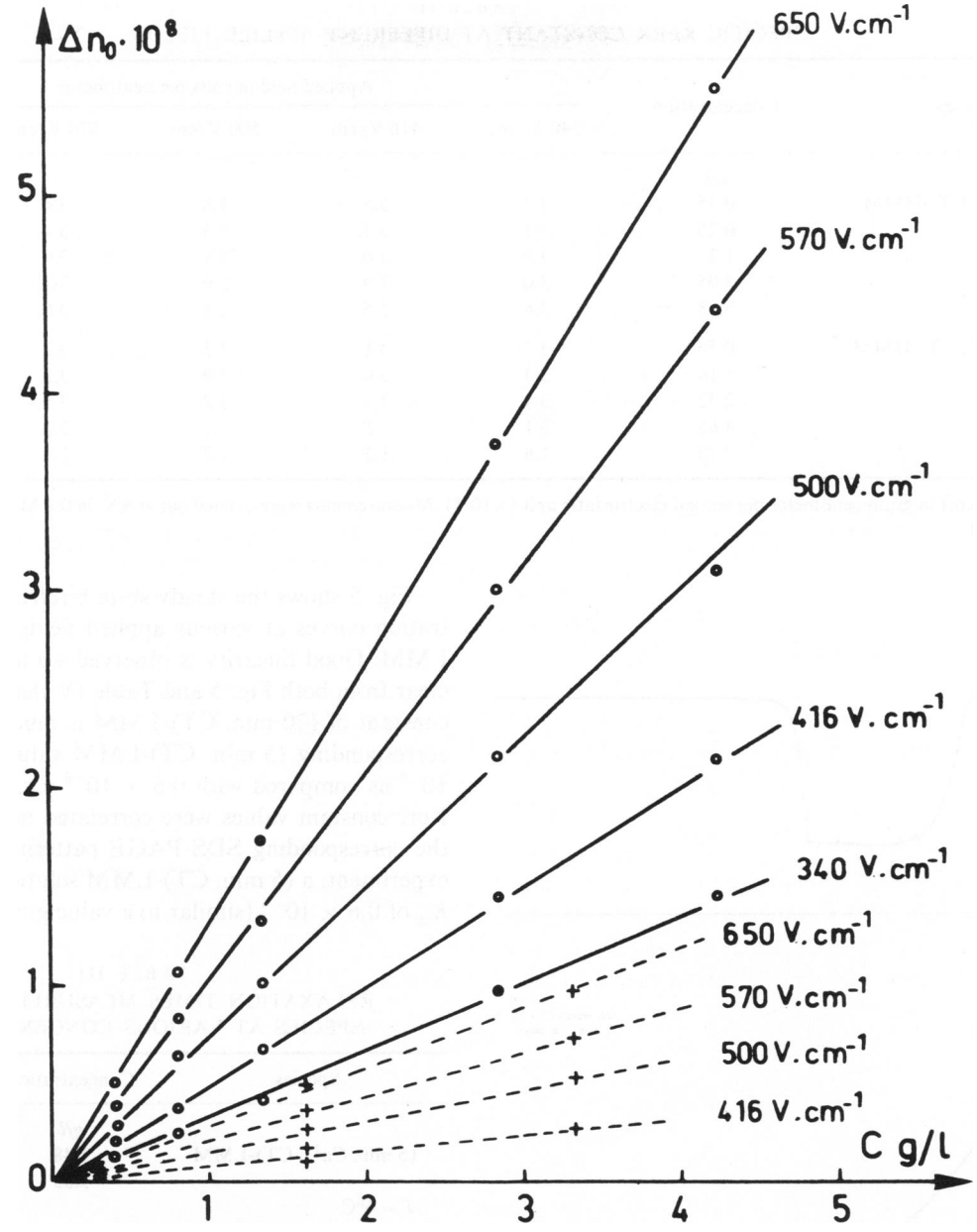

FIGURE 5 Steady state birefringence of LMM vs. concentration for various applied fields o: (20 min, Ca^{2+}, CT)-LMM; +: (5 min, Ca^{2+}, CT)-LMM. Measurements carried out under conditions as in Table I.

an independent preparation containing two bands: 71 and 62 kilodaltons in the ratio 0.42 : 0.58) was digested for 10 min with trypsin (final concentration 0.03 mg/ml; reaction stopped with soya bean trypsin inhibitor, 0.06 mg/ml). The peptide present consisted then of 62 and 55 kilodaltons in the ratio 7 : 93 and the specific Kerr constant was seen to rise to a final value of 2.4×10^{-6} c.g.s. e.s., very close to the (20 min, CT)-LMM value.

Rod

The rod portion of myosin is the whole double α-helical section of the molecule comprising LMM and S-2. SDS-PAGE analysis of the present preparations revealed a single band (Fig. 1 *g*) with minor impurities (LMM) totalling <5%. In the same buffer as that used for previous experiments birefringence signals very similar to those of LMM were obtained, showing a pure dipolar orientation and a single disorientation process (Fig. 4 *c*). Relaxation times listed in Table III are reasonably constant although a slight increase may be noticed at the higher concentrations. The rotary diffusion constant at low concentrations is $\theta_{20,w}$ = 7,300 ± 1,000 s^{-1}, significantly lower than the myosin value (9,700 s^{-1}) in spite of the fact that the molecular weight of the latter is twice as high. The steady state electric birefringence of rod solutions is plotted in Fig. 6 vs. concentration at three different applied fields. A signifi-

TABLE IV
$\Delta n/cE^2$ VALUES FOR VARIOUS MYOSIN FRAGMENTS

Species	C g/l	$\frac{\Delta n}{cE^2} \times 10^6$
(5 min, Ca^{2+}, T)-LMM	1.43	0.95
5	2.86	1.0
(5 min, Ca^{2+}, CT)-LMM C5	3.33	0.62 ± 0.05
	1.66	0.60 ± 0.1
LMM C20	4.26	2.6 ± 0.2
(20 min, Ca^{2+}, CT)-LMM	2.85	2.7 ± 0.2
	1.35	2.6 ± 0.3
	0.82	2.6 ± 0.5
	0.41	2.5 ± 0.7
(8 min, EDTA, CT)-rod	2.33	4.4 ± 0.4
	1.35	5.2 ± 0.7
	0.7	5.7 ± 0.7
	0.35	5.0 ± 0.1

$\Delta n/cE^2$ has been measured for five applied field strengths from 250 to 650 V/cm ··. Since Kerr law is correctly followed only the average values and their dispersions are given in this table.

cant saturation is found above 1.5 g/l. Table II gives the values of $\Delta n/cE^2$ for concentrations corresponding to the experimental points of the curves in Fig. 6.

Depolarized Light Scattering

Table V summarizes the results obtained with HMM and LMM solutions. The optical anisotropies γ, calculated from depolarized Rayleigh factors, are reasonably independent of solute concentrations, showing that the optical properties of myosin subfragments are not greatly

TABLE V
MOLECULAR OPTICAL ANISOTROPY γ FOR MYOSIN AND DIFFERENT TYPES OF FRAGMENTS AT VARIOUS CONCENTRATIONS

Species	Concentration	γ
	g/l	cm^3 ($\times 10^{21}$)
myosin	3.0	1.2
	0.8	1.06
(5 min, Ca^{2+}, CT)-HMM	2.5	1.15
	0.54	1.13
(20 min, Ca^{2+}, CT)-LMM	2.85	1.24
	0.85	1.13
(5 min, Ca^{2+}, T)-LMM	2.86	1.14
	0.98	1.18

influenced by molecular interactions. It is also clear that the two LMM preparations have similar optical anisotropies, the specific Kerr constant differences observed being therefore due to differences in the permanent dipole moment of the two types of molecule. The permanent dipole moments calculated from Table III are respectively: 1,800 *D* for HMM; 1,500 *D* for (5 min, Ca^{2+}, T)- and (20 min, Ca^{2+}, CT)-LMM; 900 *D* for (5 min, Ca^{2+}, CT)-LMM.

DISCUSSION

Electric birefringence can provide useful information on size (or length for rod particles) when the shape is known and a suitable model is available. Conversely, when the length of an elongated particle is assumed, the observed relaxation time can be used to derive the average shape of

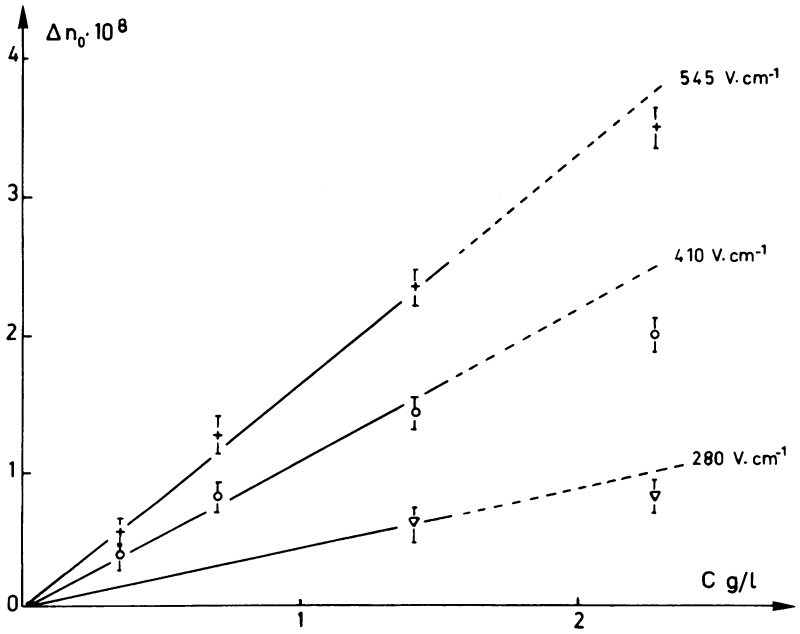

FIGURE 6 Steady state birefringence of rod vs. concentration at three different applied fields. Measurements carried out under conditions as in Table I at 17°C.

the particle in the experimental medium. The results of separate electric birefringence studies on the various myosin fragments were combined to reconstitute the myosin molecule from a scheme (described in Introduction) in which observed relaxation times were compared with calculated values based on independently determined lengths and shapes of the various fragments. However, as pointed out above, this procedure requires that the myosin fragments prepared and studied independently can be joined end to end without overlap or missing pieces between fragments or at either end. For this reason available information on fragment lengths is rapidly summarized here and compared with characteristics of our own samples.

Some of the conditions selected in the present study are expected to produce a long LMM. Our SDS-PAGE analyses show that we obtained a mixture of two strand molecular weights (71 and 62 kilodaltons). These two values agree well with other reported values for LMM, e.g.: 180–150 kilodaltons (Harrison et al., 1971); 140 kilodaltons (Lowey et al., 1969; Harrington and Burke, 1972; Akutagawa and Ooi, 1982; Waschberger and Pepe, 1980); 122 kilodaltons (Akutagawa and Ooi, 1982; Harrington and Burke, 1972; Lowey, 1971). From the molecular weight a length can be calculated by means of Crick's theoretical coordinates (1953) for a two strand coiled-coil of pure α-helix; taking 1 nm = 1.67 kilodaltons, our two species would be 85 and 74 nm long, respectively. Again this calculated value agrees reasonably well with electron microscope observations (78.5 ± 0.7 nm in Lowey et al. (1969).

Our (EDTA-CT)-rod has a molecular weight of 120 ± 5 kilodaltons, a value in good agreement with that of Weeds and Pope (1977). Using Crick's conversion factor its estimated length is 143 ± 6 nm. Other available data directly confirm this rod length as ranging from 136 ± 1.1 (Lowey et al., 1969) to 156 ± 5 nm (Elliott and Offer, 1978). An indirect S-2 length estimate is similarly derived from the M_r value of (CT)-S-2 obtained by rod digestion (Weeds and Pope, 1977), (118 kilodaltons, 70 nm). These values are consistent with those of Sutoh et al. (1978) (120 kilodaltons, 71 nm) for S-2 produced by chymotryptic digestion of (CT)-HMM similar to the HMM species used in the present study. To sum up, these comparative results indicate that: (*a*) LMM length is dependent on digestion conditions and the preparation used here is of the "long" type with a heterogeneity common to all these preparations; (*b*) S-2 in our (CT)-HMM is to a good approximation the complement of LMM with no overlap and no missing piece between these fragments; and (*c*) the rod length is certainly $\geq$140 nm.

Electric Birefringence Relaxation Times and Hydrodynamic Parameters

Previous measurements (Kobayasi and Totsuka, 1975; Highsmith et al., 1977) were carried out in denaturing media or at low ionic strength and high pH, under conditions not suitable for the evaluation of other relevant properties such as ATPase activities, filament assembly or affinity for actin. Let us first consider the hydrodynamic behavior of myosin subfragments. Two of these can be modeled to a first approximation as elongated particles (LMM and rod), whereas HMM is a rather complex structure containing two globular parts fixed onto an α-helical portion (S-2).

As seen above our LMM is a mixture of two species with lengths 85 and 74 nm calculated from molecular weights. Assuming the straight rigid rod model, the Broersma relation predicts their respective relaxation times as 8 and 12 μs (calculated at 6°C; η = 0.0147 Poises; rod diameter taken as 2 nm). Such a difference would probably be hard to detect and the experimental decay curve is reasonably fitted by a monoexponential giving a τ value of 9.3 ± 0.5 μs. If we assume a diameter of 2.0 nm for the double α-helical part of myosin (a reasonable value for a double α-helix protein and in any case of little influence in the calculation of long cylinders where $a >> b$), our electric birefringence rotary diffusion constant determination gives a length of 78 ± 2 nm for LMM in good agreement with the calculated length (79.1 ± 0.5 nm) obtained by Highsmith et al. (1977) from similar measurements carried out in 2 mM pyrophosphate at pH 9.3 using a 140 kilodalton (T)-LMM species. pH and ionic strength are thus found to have little effect on the relaxation time. The coherence observed between LMM length derived from molecular weight, electron micrograph measurements and electric birefringence support the linear rigid stick model. An important contribution of electric birefringence as compared with electron microscopy is to provide evidence for the shape of the molecule under more nearly in vivo conditions.

To interpret our experimental results with HMM and rod it is necessary to come back to previous results with myosin (Bernengo and Cardinaud, 1982). Our former determination of the rotary diffusion constant for myosin (9,700 s^{-1}) in the same buffer accounted satisfactorily for the usual LMM and rod lengths (75–85 and 140–150 nm, respectively) when an average hinge angle of 90° was used in the Garcia de la Torre and Bloomfield model (1980), consisting of an assembly of spheres and attributing to the head an approximate length of 18 nm (Elliott and Offer, 1978). Although our observed relaxation time ($\tau_{20,w}$ = 17 ± 2 μs) was shorter than the calculated Garcia de la Torre and Bloomfield value (20 μs) the agreement is close enough to lend strong support to the myosin model with an average 90° angle at the HMM-LMM junction. The Garcia de la Torre and Bloomfield model was also used to calculate relaxation times of HMM's with various S-2 lengths assuming an average value over five orientation angles of S-1 heads relative to each other. The best fit to our results corresponds to an S-2 length of 72 nm. This value compares favorably with S-2 lengths (70–71 nm)

calculated from M_r values (Weeds and Pope, 1977; Sutoh et al., 1978). On the other hand Kobayasi and Totsuka (1975) report an HMM relaxation time value (5 μs) from which the Garcia de la Torre and Bloomfield model yields an S-2 length of ~50 nm. No detailed information is available on their preparation but it may be assumed that the procedure used produced essentially a "short" HMM, i.e., an HMM species with a short S-2. A seemingly weak point at this stage is that with the Garcia de la Torre and Bloomfield model a number of parameters such as average angle between the heads and dimension of the head are accepted as invariants inherent to the model. However, this is justified considering that: (*a*) standard deviations calculated for four or five different orientations of the heads represent ~10% of the average value; (*b*) the observed τ_0 difference between our HMM and that of Kobayasi and Totsuka is fully accounted for by the suspected difference in S-2 length.

The rod length is therefore (78 + 72) nm = 150 nm from our electric birefringence data on LMM and HMM, in good agreement with values (136–156 nm) derived from molecular weight values or electron micrograph measurements (see first part of Discussion). Assuming the rod to be fully extended its rotary diffusion constant calculated from Broersma's equation would be 4,400 s^{-1}, significantly below our present experimental value of 7,300 ± 1,000 s^{-1}. A reasonable explanation is that rod as demonstrated for myosin tail, can best be represented as a broken stick. The calculated hydrodynamic properties for various rod models of variable bend angle and assumed length of 144–150 nm indicate that our experimental $\theta_{20,w}$ value corresponds to an average bend angle certainly >90° and <180° and a reasonable estimate lies between 120 and 135°. Highsmith et al. (1977), in 2 mM pyrophosphate at pH 9.3, observed relaxation times longer than those discussed here, but also conclude that a statistically bent rod must be assumed to account for the recorded relaxation times. A subsequent determination by depolarized light scattering measurement in a high ionic strength medium in the presence of 0.01 M pyrophosphate at pH 9.5 gave a bend angle of 128° (Highsmith et al., 1982). It is thus clearly established that rod is more elongated than myosin in the same solvent. This could be due either to an influence of the head structure on an elastic restoring force at the HMM-LMM hinge or simply to the fact that asymmetry in myosin somehow stabilizes the more compact bent structure. A precise temperature-dependence study of τ in myosin and rod should clear up this point.

Electric birefringence data are coherent with known "morphological" characteristics of myosin and rod and supply independent evidence of flexibility at the HMM-LMM hinge, showing also that in solution the preferred tail conformation is not the straight rod. The model used takes S-2 as fully elongated. The satisfactory agreement between values derived from our HMM study as compared to S-2 lengths from other sources shows that a possible S-2 flexibility (Highsmith et al., 1977); a study at pH 9.3 in 2 mM pyrophosphate) is not detected by electric birefringence measurements of HMM at physiological pH. On the other hand, if the flexible part of S-2 makes up the hinge (Lu, 1980) the putative bending of this COOH-terminus segment in HMM is not expected to reduce the HMM relaxation time significantly.

Molecular Interactions

In the present concentration range LMM seems not to aggregate noticeably since no significantly longer relaxation time can be detected in the birefringence decays (43 nm staggered dimers, 121 nm total length, would yield a relaxation time of ~23.9 μs instead of 6.4 μs for the monomer), hence parallel staggered dimers, if any, contribute no more than 2% of the total signal in a 5 mg/ml solution. The possible formation of side by side nonstaggered aggregates is more difficult to exclude since the relaxation time of these aggregates is expected to be barely longer than that of monomers. However, they should lead to an increase in the specific Kerr constant if parallel and a decrease if antiparallel; this is not the case in the present experiment, birefringence being proportional to concentration up to 7 g/1.

The situation is not so clear for HMM and rod because a saturation effect (decrease in the apparent specific birefringence) becomes visible at high concentrations. This saturation can have at least two origins: (*a*) some intermolecular interactions occur when the molecules are close together (electrostatic or dipole-dipole interactions); (*b*) antiparallel association takes place in the solution, decreasing the quantity of oriented monomers per unit volume (anti-parallel side-by-side nonstaggered aggregates should have a very weak permanent dipole moment as compared with monomers). In such a case examination of Table II shows for HMM a K_{sp} decrease of the order of 10% for a concentration of 7.6 g/1; assuming a dimeric association this value corresponds to an equilibrium constant of the order of 0.1 deciliter/g. For rod the equilibrium constant would be higher (0.5 deciliter/g).

Thus the expected staggered LMM and rod dimers, which would result in a biexponential decay curve, have not been detected in the present solutions. In any case their autoassociation constant assumes values much lower than those determined by sedimentation equilibrium and sedimentation velocity (Harrington and Burke, 1971). HMM is not expected to autoassociate into any kind of well defined dimer, hence only intermolecular electrostatic or diple-dipole interaction can be suspected with this species. On the other hand it is not possible to exclude the occurrence of anti-parallel nonstaggered rod dimers. However, this species has no apparent biological significance since in thick filament the myosin molecules are found in either parallel or anti-parallel staggered arrangements.

Kerr Constant Variations

The Kerr constant variations of LMM as observed here illustrate the potential usefulness of this parameter. Although an apparent homogeneity of myosin subfragments has been shown by equilibrium centrifugation (Margossian et al., 1981), SDS-PAGE is often used to reveal nonhomogeneity in either the extent of internal cleavages or the nibbling of extremities (Cardinaud et al., 1973; Weeds and Pope, 1977; Highsmith, 1977; Cardinaud, 1981; Yagi and Offer, 1981; Akutagawa and Ooi, 1982). Similarly the decay curves are found here to be well fitted by a single relaxation time (also a good indication of homogeneity) whereas very large Kerr constant variations reveal subtle differences in the constituent peptides. The two LMM of length 85 and 74 nm detected by SDS-PAGE have been shown to give an apparent single birefringence decay. On the other hand the electro-optical method used here appears to be extremely sensitive in detecting slight differences due to nibbling at the ends of elongated molecules considering the possible change in the molecule dipole moment. The removal of one charged amino acid at the end of the LMM subfragment is enough to alter the dipole moment by ~2,000 Debye. Such a pinpoint modification would be barely detectable by conventional biochemical methods, whereas peptide analysis and electric birefringence combined may give access to experimental determination of net charge distribution. With LMM in particular this point is important since a segment close to the COOH-terminus is held responsible for insolubility (Akutagawa and Ooi, 1982; Nyitray et al., 1983) and is therefore suspected to be a key element in filament formation, the staggering being such that oppositely charged zones mutually interact to organize and stabilize the filament (McLachlan and Karn, 1982). In our LMM species for example the cleavage possibilities as offered by chymotrypsin are as follows: Phe-450---Phe-471---Phe-612---Tyr-623--Tyr-1015---Tyr-1040---Phe-1059---Glu-COOH-1098 using the rod sequence and numbering of McLachland and Karn (1982). The apparent weight difference recorded between the two main strands found in (5 min, Ca^{2+}, CT)-LMM (~9 kilodaltons) is consistent with a break at Tyr-1015, severing a COOH-terminal segment of (~8.5–9.0 kilodaltons) and saving the ~5 kilodaltons peptide essential for insolubility properties of LMM (Nyitray et al., 1983). Prolonged proteolysis leads to a decrease in the proportion of the 71 kilodalton strand, together with an observed increase in the permanent dipole moment. Since the dipole moment is increased by the loss of a COOH-terminal segment having a slight excess of positive charge our longer LMM appears to be a dipole with a net negative charge on the C-terminus and a net positive charge on the N-terminus oriented as: ^{+}N-----C^{-}, assuming that removal of the segment causes no polarity inversion, which is a possibility not to be discarded at the present time.

Note added in proof: Other models could have been examined, such as a semi-flexible model (S. Hvidt, F. H. M. Nestler, M. L. Greaser, and J. D. Ferry, 1982, *Biochemistry.* 21:4064–4073) or a segmented model (W. A. Wegener, 1982, *Biopolymers.* 21:1049–1080). We based our interpretation mainly on the Garcia de la Torre and Bloomfield model because of its success in explaining electric birefringence results obtained earlier with similar systems (C. Marion, P. Bezot, C. Bezot, B. Roux, and J. C. Bernengo, 1981, *Eur. J. Biochem.* 120:169–176.

Received for publication 9 April 1984 and in final form 24 January 1985.

REFERENCES

Akutagawa, T., and T. Ooi. 1982. Fragments responsible for the low solubility of light meromyosin obtained by limited proteolysis. *J. Biochem. (Tokyo).* 92:999–1007.

Bailey, J. L. 1967. *In* Techniques in Protein Chemistry. Elsevier/North Holland, Amsterdam. 340–352.

Balint, N., L. Szilagyi, N. Blazso, and N. A. Biro. 1968. Studies on proteins and protein complexes of muscles by means of proteolysis V. Fragmentation of light meromyosin by trypsin. *J. Mol. Biol.* 37:317–330.

Bernengo, J. C., and R. Cardinaud. 1982. State of myosin in solution. Electric birefringence and dynamic light scattering studies. *J. Mol. Biol.* 159:501–517.

Bernengo, J. C., B. Roux, and M. Hanss. 1973. Electric birefringence apparatus for conducting solutions. *Rev. Sci. Inst.* 44:1083–1086.

Bernengo, J. C., B. Roux, and D. Herbage. 1974. Electric birefringence study of monodisperse collagen solutions. *Biopolymers.* 13:641–647.

Broersma, S. 1960. Rotational diffusion constant of a cylindrical particle. *J. Chem. Phys.* 32:1626–1631.

Cardinaud, R. 1979. Proteolytic fragmentation of myosin: location of SH-1 and SH-2 thiols. *Biochimie.* 61:807–821.

Cardinaud, R. 1980. Fate of the light chains in the course of proteolytic digestion of rabbit fast skeletal myosin. *Biochimie.* 62:135–245.

Cardinaud, R., E. Dassin, and F. Pelletier. 1973. Heterogeneity of subfragment-1 preparations from myofibril digestion by trypsin. *Biochem. Biophys. Res. Commun.* 52:1057–1063.

Cardinaud, R., and M. Drifford. 1982. Quasi-elastic light scattering studies of rabbit skeletal myosin solutions. *J. Muscle Res. Cell Motil.* 3:313–332.

Craig, R., R. Smith, and J. Kendrick-Jones. 1983. Light chain phosphorylation controls the conformation of vertebrate non-muscle and smooth muscle myosin molecules. *Nature (Lond.).* 302:436–439.

Crick, F. H. C. 1953. The packing of α-helices: simple coiled-coils. *Acta Crystallogr.* 6:689–697.

Elliott, A., and G. Offer. 1978. Shape and flexibility of the myosin molecule. *J. Mol. Biol.* 123:505–519.

Franck, G., and A. G. Weeds. 1974. The amino acid sequence of the alkali light chains of rabbit skeletal muscle myosin. *Eur. J. Biochem.* 44:317–334.

Fredericq, E., and C. Houssier. 1973. Electric dichroism and electric birefringence. Clarendon Press, Oxford, England.

Garcia de la Torre, G., and V. A. Bloomfield. 1980. Conformation of myosin in dilute solutions as estimated from hydrodynamic properties. *Biochemistry.* 19:5118–5123.

Godfrey, J. A., and W. F. Harrington. 1970. Self-association in the myosin systems at high ionic strength. I. Sensitivity of the interaction to pH and ionic environment. *Biochemistry.* 9:886–893.

Harrington, W. F. 1979. Contractile proteins of muscle. *In* The Proteins. H. Neurath and R. L. Hill, editors. Academic Press, Inc., New York. 4:246–411.

Harrington, W. F., and M. Burke. 1972. Geometry of the myosin dimer in high salt media. Association behavior of rod segments from myosin. *Biochemistry.* 11:1448–1455.

Harrison, R. G., S. Lowey, and C. Cohen. 1971. Assembly of myosin. *J. Mol. Biol.* 59:531–535.

Harvey, S. C., and M. C. Cheung. 1977. Fluorescence depolarization studies on the flexibility of myosin rod. *Biochemistry.* 16:5181–5187.

Highsmith, S. 1981. The dynamics of myosin and actin in solution are compatible with the mechanical features of the cross-bridge hypothesis. *Biochem. Biophys. Acta.* 639:31–39.

Highsmith, S., and O. Jardetzky. 1981. Internal motions in myosin. *Biochemistry.* 20:780–783.

Highsmith, S., M. Kretzschmar, C. T. O'Konski, and M. F. Morales. 1977. Flexibility of myosin rod, light meromyosin and myosin subfragment-2 in solution. *Proc. Natl. Acad. Sci. USA.* 74:4986–4990.

Highsmith, S., C. C. Wang, K. Zero, R. Pecora, and O. Jardetzky. 1982. Bending motions and internal motions in myosin rod. *Biochemistry.* 21:1192–1197.

Huxley, A. F., and R. M. Simmons. 1971. Proposed mechanism of force generation in striated muscle. *Nature* (*Lond.*). 233:538–539.

Huxley, H. E. 1963. Electron microscope studies on the structure of natural and synthetic protein filaments from striated muscle. *J. Mol. Biol.* 7:281–308.

Huxley, H. E. 1969. The mechanism of muscular contraction. *Science* (*Wash. DC*). 164:1356–1366.

Kahn, L. D. 1972. Electric birefringence. *In* Enzyme Structure. C. H. Hirs and S. Timasheff, editors. *In* Methods in Enzymology. S. P. Colowick, and N. O. Kaplan, editors. Academic Press, Inc., London. 26:323–337.

Kobayasi, S., and T. Totsuka. 1975. Electric birefringence of myosin subfragments. *Biochem. Biophys. Acta.* 376:375–385.

Lowey, S. 1971. Myosin: molecule and filament. *In* Subunits in Biological Systems. Part A. S. N. Timasheff and G. D. Fassman, editors. Marcel Dekker, Inc., New York. 202–260.

Lowey, S., H. S. Slayter, A. G. Weeds, and H. Baker. 1969. Substructure of the myosin molecule. I. Subfragments of myosin by enzymic degradation. *J. Mol. Biol.* 42:1–29.

Margossian, S. S., W. F. Stafford III, and S. Lowey. 1981. Homogeneity of myosin subfragments by equilibrium centrifugation. *Biochemistry.* 20:2151–2155.

MacLachland, A. D., and J. Karn. 1982. Periodic charge distribution in the myosin rod amino acid sequence match cross-bridge spacing in muscle. *Nature* (*Lond.*). 299:226–231.

Miyahara, M., and H. Noda. 1979. Electric and flow birefringence properties of myosin in aqueous urea and sodium pyrophosphate. *J. Biochem.* 86:239–248.

Montague, C., and F. D. Carlson. 1982. Preparation of contractile proteins for photon correlation spectroscopy and classical light scattering studies. *In* The Contractile Apparatus and the Cytoskeleton. D. W. Frederiksen and L. W. Cunningham, editors. *In* Methods in Enzymology. S. P. Colowick and N. O. Kaplan, editors. Vol. 85 part B. Academic Press, Inc., New York. 562–570.

Nyitray, L., G. Mocz, L. Szilagyi, M. Balint, R. C. Lu, A. Wong, and J. Gergely. 1983. The proteolytic structure of light meromyosin. Localization of a region responsible for the low ionic strength insolubility of myosin. *J. Biol. Chem.258:13213–13220.*

Parry, D. A. D. 1981. Structure of rabbit skeletal myosin. Analysis of the amino acid sequences of two fragments from the rod region. *J. Mol. Biol.* 153:459–464.

Sarkar, J. 1973. Stoichiometry and sequential removal of the light chains of myosin. *In* The Mechanism of Muscle Contraction. *Cold Spring Harbor Symp. Quant. Biol.* 37:14–17.

Sutoh, K., T. Karr, and W. F. Harrington. 1978. Isolation and physicochemical properties of a high molecular weight subfragment-2 of myosin. *J. Mol. Biol.* 126:1–22.

Szent-Gyorgyi, A. G., C. Cohen, and D. E. Philpott. 1960. Light meromyosin fraction I: a helical molecule from myosin. *J. Mol. Biol.* 2:133–142.

Takahashi, K. 1978. Topography of the myosin molecule as visualized by an improved negative staining method. *J. Biochem.* 13:905–908.

Trybus, K. M., T. W. Huiatt, and S. Lowey. 1982. A bent monomeric conformation of myosin from smooth muscle. *Proc. Natl. Acad. Sci. USA.* 79:6151–6155.

Waschberger, P. R., and F. A. Pepe. 1980. Interaction between vertebrate skeletal and uterine muscle myosins and light meromyosins. *J. Cell Biol.* 85:33–41.

Weeds, A. G., and B. Pope. 1977. Studies on the chymotryptic digestion of myosin. Effects of divalent cations on proteolytic susceptibility. *J. Mol. Biol.* 111:129–157.

Weeds, A. G., and R. S. Taylor. 1975. Separation of subfragment-1 isoenzymes from rabbit skeletal myosin. *Nature* (*Lond.*). 257:54–56.

Yagi, N., and G. W. Offer. 1981. X-ray diffraction and electron microscopy of a light meromyosin tactoid. *J. Mol. Biol.* 151:467–490.